

A stereoscopic approach for three dimensional tracking of marine biofouling microorganisms

S. Maleschlijski¹, L. Leal-Taixé², S. Weiße³, A. Di Fino⁴, N. Aldred⁴, A. S. Clare⁴, G. H. Sendra³,
B. Rosenhahn² and A. Rosenhahn^{1,3}

¹Institute of Functional Interfaces, Karlsruhe Institute of Technology, PO Box 3640, 76021 Karlsruhe, Germany

²Leibniz University Hannover, Appelstr. 9A, Hannover, Germany

³Applied Physical Chemistry, Ruprecht-Karls-University Heidelberg, INF 253, 69120 Heidelberg, Germany

⁴School of Marine Science and Technology, Newcastle University, Newcastle upon Tyne NE1 7RU, UK

Abstract—The extraction and analysis of three dimensional tracking data relating to surface exploration of sessile marine organisms is of great importance for understanding the mechanism of surface colonization (biofouling). The knowledge of behavior can thus be used to develop tools for controlling and influencing undesirable impacts that arise as a consequence of the adhered organisms. This paper describes a stereoscopic system currently in development for tracking barnacle cyprids and allows extraction of 3D swimming patterns for a common marine biofouling organism - *Semibalanus balanoides*. The details of the hardware setup and the calibration object are presented and discussed. In addition we describe the algorithm for the camera calibration, object matching and stereo triangulation. As practical result, several trajectories of living cyprids are presented and analyzed with respect to statistical swimming parameters.

I. INTRODUCTION

The term biofouling describes the unwanted accumulation of biomass on surfaces [1]. The macroscopically visible consequences have severe effects on frictional drag and lead to higher fuel consumption of vessels [2]. Barnacles are one of the most prevalent marine fouling species and contribute significantly to increased hydrodynamic drag [2]. The problem is currently revisited as tributyltin (TBT) based coatings, the former work horse of the marine coating industry, are being banned and thus researchers seek alternatives. To inform the development of environmentally benign coating strategies it is important to understand the colonization mechanisms of the target organisms. Thus, we aim to better understand the initial phase of barnacle colonization, which occurs via their larvae, the cyprids. 2D tracking has already been used to derive statistical data from cyprid tracks [3]. However, the three-dimensional nature of the motion makes it difficult to distinguish swimming from exploring cyprids. One technique which was found to be highly useful for 3D tracking is digital in-line holography [4], [5], [6], [7], [8], [9]. This method is unique and brings very good results when objects smaller than 300-400 μm are investigated. The raw data is in the form of a hologram, which needs to be processed with complex, time consuming algorithms in order to reconstruct the whole stack of three dimensional images. Specific methods have been

presented for tracking [10] and pattern classification [11] for this type of data.

The application of a stereoscopic system with objects of some micrometers or even nanometer sizes is mechanically and optically very difficult to realize. On the other hand when the target objects are bigger, stereoscopy offers the more efficient solution. Since cyprids are much larger compared to the microorganisms commonly used for holography, we present a stereoscopic system which allows 3D trajectories of barnacle cyprids to be visualized and statistically analyzed. An overview on the whole project is shown in figure 1.

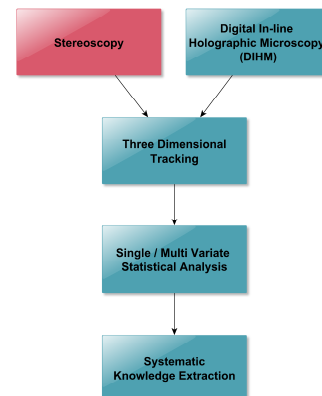


Figure 1. Project overview: Extracting statistical data on motility from three dimensional swimming trajectories.

In this paper, we describe the technical approach for obtaining 3D swimming trajectories of marine biofouling organisms, applying stereo-triangulation and automatic particle matching algorithms, the hardware setup, the calibration procedure, as well as the image processing techniques applied to obtain first trajectories.

II. METHODS

A. Hardware setup

By definition stereoscopy needs at least two different viewing angles in order to solve the third dimension ambiguity.

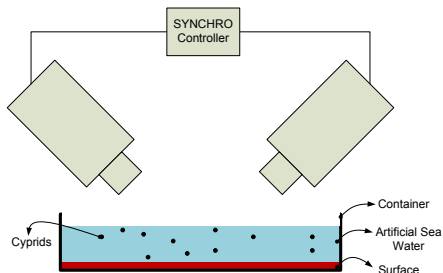


Figure 2. Schematic view of the setup used for the measurements, consisting of two cameras, synchronization controller, a container with artificial sea water, test microorganisms and an experimental surface.

The number of cameras applied as well as the viewing angle depends on the density of the particles/microorganisms to be distinguished. The setup developed in this work used two consumer cameras, since only a small number of microorganisms were observed simultaneously. The experiments were conducted with two high definition Sony cameras at a viewing angle of 60-89 degrees. Figure 2 shows a schematic view of the setup.

One important requirement for the object matching and triangulation algorithms is to have two temporally synchronized video sequences. The following synchronization techniques were discussed:

- *Temporal synchronization using video markers:* In this case the two cameras are started manually and a short, bright flash is used to mark the start of the video. In the post processing step, the user manually adjusts the frames of both cameras according to the video marks.
- *Temporal synchronization using audio markers:* Here the two cameras are started manually again and a short, loud and easily detectable audio mark is used to mark the start of the recording [12]. In the post processing step, the user manually adjust the frames of both cameras according to the audio marker.
- *Temporal synchronization using external shared trigger:* In this technique an external trigger signal is used to start the recording sequence in a synchronized manner.

The last technique was applied in the current experiment, using a stereo LANC remote controller (ste-fra LANC V3.0M, digi-dat). The controller offers a hardware synchronization with a small synchronization error of up to 2 ms. This mis-synch value proved to be acceptable for our experiments, because at a frame rate of 25 fps, it corresponds to 0.05 frames. Figure 3 shows the model and example images of the calibration object used in the experiments.

The calibration object has 128 points (back-illuminated holes with a diameter of 1 mm) distributed across four planes. It is designed with the same dimensions as an objective slide and can after calibration simply be exchanged by the coated objective slide. In the next section, we detail the image processing techniques used to extract the 2D positions of the organisms on both images and how the 3D trajectories are reconstructed using the projection matrices. For more

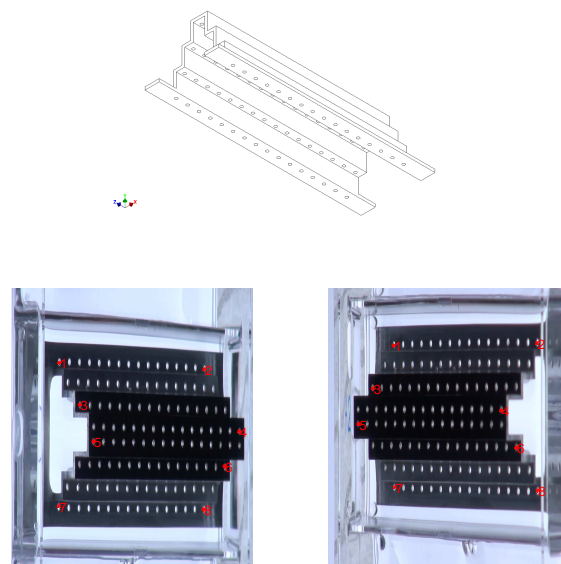


Figure 3. Top: Calibration object containing points in four planes, providing sufficient individual positions for mathematical determination of the unknown transformation parameters. Bottom: Images of the calibration cube in the media and selected points for calibration.

information on 3D reconstruction and epipolar geometry, we refer to [13].

The workflow of our developed algorithm as described in the next subsections is summarized in figure 4.

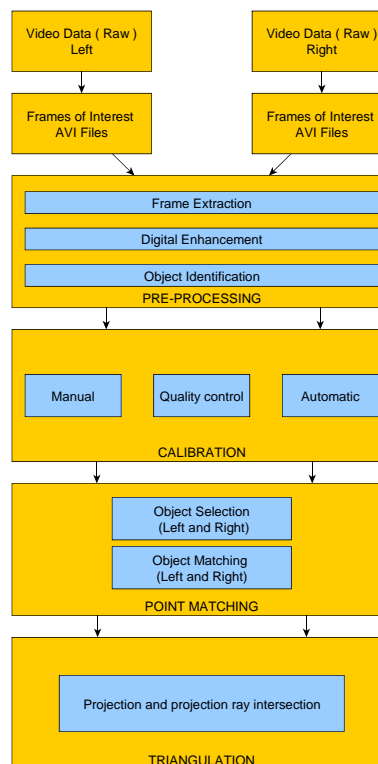


Figure 4. Algorithm for the extraction of the three dimensional data.

B. Particle detection and 3D trajectory reconstruction

The particles are detected by a simple thresholding using a previously recorded background image. The detected areas of sufficient size are then selected as particles for tracking. The tracking algorithm used [10] will deal with missing particles and false alarms.

Once 2D points are found, we need to obtain the relation between the detected 2D point in the camera and its real 3D position. This relation is given by the projection matrix P , which contains information about the camera position, internal parameters and geometry of the setup. Using a set of known 3D points X_n and their projection on the image planes x_n , it is possible to calculate the projection matrix as direct linear transform (DLT) for the left and right imaging device by optimizing a linear system of equations of the form

$$x_n \times P \cdot X_n = 0 \quad (1)$$

for each camera for $n > 6$ correspondences which have to be found manually on each image.

For any homogeneous 2D point x and corresponding 3D point X , the relation $x \doteq PX$ holds. The projection matrix can be divided into extrinsic \mathbf{R} and intrinsic \mathbf{K} parameters as follows:

$$P = \underbrace{\begin{pmatrix} k_u f & 0 & u_0 \\ 0 & k_v f & v_0 \\ 0 & 0 & 1 \end{pmatrix}}_{\mathbf{K}} \underbrace{\begin{pmatrix} r_{11} & r_{12} & r_{13} & t_1 \\ r_{21} & r_{22} & r_{23} & t_2 \\ r_{31} & r_{32} & r_{33} & t_3 \end{pmatrix}}_{\mathbf{R}} \quad (2)$$

where k_u and k_v are the pixels per unit of distance in pixel coordinates, f is the focal length and (u_0, v_0) is the principal point. \mathbf{R} contains the joint rotation-translation matrix, called a matrix of extrinsic parameters. It translates coordinates of a point to some coordinate system, fixed with respect to the camera.

Once the calibration is done and we obtain the projection matrix, we can project any 2D point to a 3D projection ray. If we do this on both cameras, the intersection of both projection rays will give us the 3D position of the particle. The complete process of 3D reconstruction is detailed below.

First, by using the respective projection matrix, all image points in the left and right camera are reconstructed to 3D projection rays by simple back-projection. The 3D lines are reconstructed in *Pluecker coordinates* [14], an efficient implicit 3D line representation which allows for easy computation of point/line distances: A Pluecker line $L = (n, m)$ is given by a normalized 3D vector n (the direction of the line) with $\|n\| = 1$ and a 3D vector m , called the moment, which is defined by $m := x' \times n$ for a given point x' on the line. Collinearity of a point x to a line L can be expressed by

$$x \in L \Leftrightarrow x \times n - m = 0, \quad (3)$$

and the distance of a point x to the line L can easily be computed by $\|x \times n - m\|$.

The intersection of two lines $L_1 = (n_1, m_1)$ and $L_2 = (n_2, m_2)$ can be computed as

$$\begin{aligned} X &= L_1 \wedge L_2 \\ &= \left(\frac{n_1 \cdot (n_2 \times m_2)}{\|n_1 \times n_2\|^2} - \frac{(n_1 \cdot n_2)(n_1 \cdot (n_2 \times m_1))}{\|n_1 \times n_2\|^2} \right) n_1 + \\ &\quad (n_1 \times m_1) \end{aligned} \quad (4)$$

Note, that equation (4) results in a point on the first line L_1 which is closest to the second line L_2 . For skewed lines, we simply compute the closest point between both lines as

$$X_C = 0.5 \cdot (L_1 \wedge L_2 + L_2 \wedge L_1). \quad (5)$$

To obtain the correspondences between detected particles in both cameras we generate a cost matrix $C = C(i, j)$ which contains the distances between line i and line j by reconstructing the 3D point X using equation (4) and computing the distance to the projection rays by evaluating $C(i, j) = \|X \times n_i - m_i\| + \|X \times n_j - m_j\|$. The correspondences are then found using the Hungarian graph matching algorithm [15], which provides the globally optimal matches for a given C . The outcome are the corresponding particles between the right and left camera which are then reconstructed using equation (4).

As a simple test we reconstructed a couple of back-projected 3D points in figure 5. Even though we do not take into account lens distortion or the refraction index of the media, the 3D reconstruction is pretty accurate (mean deviation is 0.0499 millimeters in 3D-space) and sufficient for our studies.

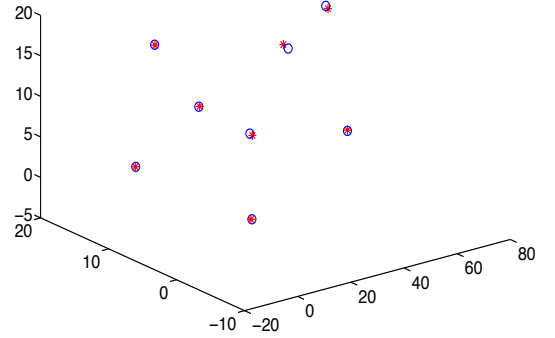


Figure 5. 3D-points (shown in blue) have been projected onto the image plane and are reconstructed as further 3D-points (shown in red). The mean deviation is 0.0499 millimeters.

Once the 3D positions of all the particles are found, we make use of the system described in [10], which uses the multi-level Hungarian to obtain the full 3D trajectories in time. The system deals with entering and leaving particles, as well as missing data and false alarms, and has been proven to work for fast moving microorganisms.

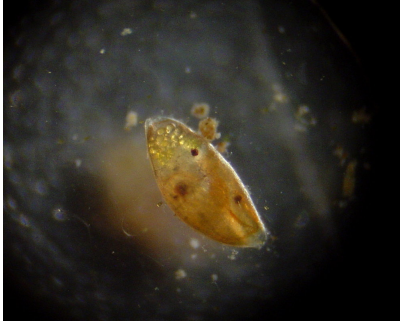


Figure 6. *Semibalanus balanoides* with typical sizes of 700-1300 μm [16] (Reprint permission kindly provided by J. O. Bjørndal [17]).

III. EXPERIMENTS

The described system was applied for the tracking of the barnacle cyprids *Semibalanus balanoides* in experiments carried out at the School of Marine Science and Technology, Newcastle University, United Kingdom.

In a series of experiments surfaces with different coating properties were tested. There were two big groups of surface coatings - having an attractive effect on the microorganisms and having a repulsive effect on them. Once the target surfaces and microorganisms have been selected and the cameras, the light source and the container have been aligned as shown in the figure 2, calibration measurements were carried out followed by a tracking experiment.

1) Calibration Measurement Phase

- a) In order to be able to calculate a model including the full influence of the multi-media environment (air, container wall, water, lens distortions) the calibration object is placed in the container in the same manner as later on the test surfaces.
- b) A short video (used to extract a calibration frame) is recorded in order to have enough calibration data for both imaging devices.

2) Measurement Phase

- a) The new test surface is placed in the container in order to provoke real-life swimming patterns in the microorganisms.
- b) The cyprids are then inoculated, and given 5 minutes to adapt to a possible water temperature change.
- c) A 45 minute video of the swimming cyprids is recorded with the left and right camera.

3) Data processing Phase

- a) Pre-processing: The data is pre-processed in order to get better quality images, which are used for the extraction of the positioning data.
- b) Calibration parameter calculation: After the frame data is available, the calibration procedure is applied in order to calculate the mathematical models for both cameras.
- c) Point matching: Knowing the camera models and using the epipolar geometry the point matching algorithm is used in order to identify potential point pairs in the frames of the left and right camera.

- d) Triangulation: Once the point pairs for all objects of interest in the frames are known, the camera models are used to create projection rays. The crossing point of the projection rays is the three-dimensional coordinate of the object of interest in real-life coordinates.

4) Tracking Phase

The connected three dimensional coordinates of the objects of interest from all of the frames represent the traces in the video sequence.

5) Analysis Phase

The traces are then statistically analyzed in order to extract the systematic knowledge over the behavior of the *Semibalanus balanoides* in vicinity of the target surface.

IV. RESULTS

Figure 7 shows five traces of cyprids, exploring a glass surface. There are 250 measurement points used to generate each trace, which at a frame rate of 25 fps corresponds to 10 seconds of the recorded video material. With statistical tools it is possible to extract behavioral parameters [5], describing the changes in swimming patterns [11] depending on the type of surface in the container.

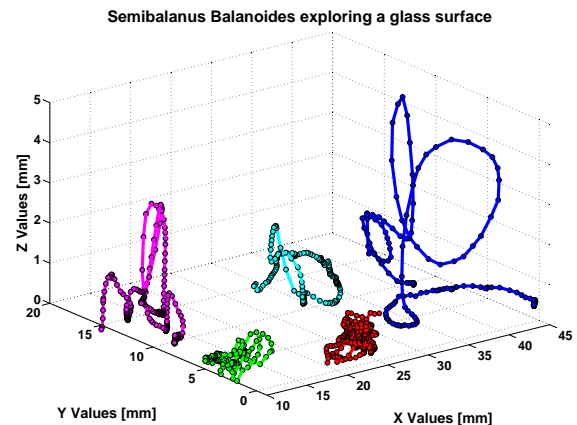


Figure 7. Sample trajectories of *Semibalanus balanoides* exploring a glass surface.

Figure 8 and 9 describe the occurrence of the different swimming velocities in the measured trajectories. In general the observed speeds are in line with recent investigation of Marechal et al. [3] with velocities in the order of $\sim 10\text{-}15$ mm/s. In figure 8 it is visible, that there is a high occurrence of velocities close to zero, which correspond to non moving cyprids. These occasional stops are characteristic for the swimming motion of the cyprids.

In figure 9 the individual histograms of the trajectories from figure 7 are presented. For better visibility of the distribution of the velocity of the swimming cyprids, the velocities which correspond to a non moving cyprid (velocity values lower than 1 mm/s) were not used for the calculation.

Although the mean velocity of the swimming cyprids is between $\sim 10\text{-}15$ mm/s in all five histograms, there are some

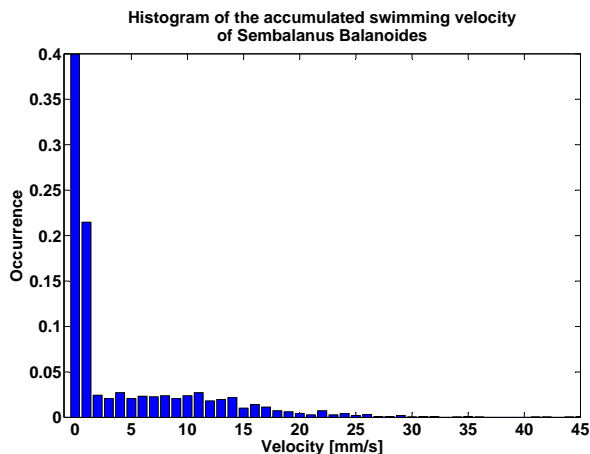


Figure 8. Histogram of the accumulated swimming velocity of the five *Semibalanus balanoides* traces.

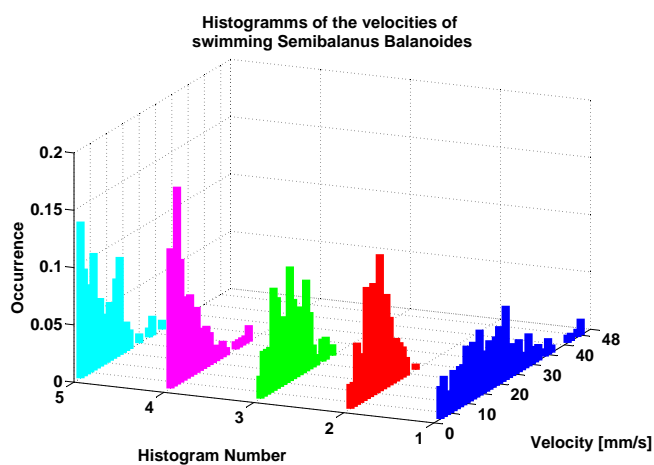


Figure 9. Single histograms of the velocity of swimming *Semibalanus balanoides* (velocities lower than 1 mm/s were defined to be of a static cyprid and were not used for calculation of the histograms).

features which are slightly different and can be categorized in three groups:

- The blue colored cyprid trace (Figure 9, Histogram 1) shows predominantly swimming behavior and uses a swimming depth of 6 mm in the z-direction. Maximum velocities of up to 45 mm/s are observed. The motion pattern seems to be typical for free swimming.
- The magenta and cyan colored traces (Figure 9, Histogram 4, 5) show swimming behavior with sporadic surface contacts. The trajectories seem to indicate a phase in which cyprids explore the surface and occasionally probe it in greater detail.
- The red and green colored traces (Figure 9, Histogram 2, 3) show cyprids which are nearly the whole time at a certain position and seem to intensely explore a specific site. Such sites could be ones which are interesting and potentially suited for permanent attachment.

V. CONCLUSIONS AND FUTURE WORK

We present a stereoscopic setup suited for tracking of sub-micrometer sized microorganisms and the conducted experiments allow to accurately extract trajectories. The resolution is limited only by the resolution of the camera equipment used and the angle in which the two cameras are aligned. One big advantage of the presented algorithm is that it allows a label-free tracking of moving particles with conventional cameras. In addition the algorithm is capable of tracking multiple moving objects of interest simultaneously.

In the first tests the hardware setup and the algorithms proved to be working very well. The future work can be divided into two parts - biological and algorithmic. In the next step on the biological side systematic tests of surfaces with different properties and different microorganisms will be conducted in order to obtain statistically relevant quantitative data on barnacle cyprid exploration behavior. The derived knowledge allows to understand settlement and selection strategies and thus offers opportunities to interfere in order to develop new routes towards environmentally benign antifouling approaches. On the algorithmic side, the effects of the multi-media environment (air, plastic, water, glass, etc.) will be investigated and new image processing techniques will be applied to enhance the image contrast. In the last phase of the future work an underwater setup will be designed, constructed and tested in the natural habitat of the biofouling microorganisms - the ocean.

VI. ACKNOWLEDGMENTS

This work was funded by the following projects: DFG Ro 2524/2-2, Ro 2497/7-2, ONR N00014-08-1-1/16 and Sea-coat (Marie Curie ITN). We thank S. Conlan (University of Newcastle) for her support and suggestions in the biological experiments and I. Thomé (University of Heidelberg) for surface preparation.

REFERENCES

- [1] R.L. Townsin, "The ship hull fouling penalty," *Biofouling*, vol. 19 (Suppl.), pp. 9–15, 2003.
- [2] M.P. Schultz, "Effects on coating roughness and biofouling on ship resistance and powering," *Biofouling*, vol. 23(5), pp. 331–341, 2007.
- [3] J.P. Marechal, C. Hellio, M. Sebire, and A.S. Clare, "Settlement behaviour of marine invertebrate larvae measured by EthoVision 3.0," *Biofouling*, vol. 20(4-5), pp. 211–217, 2004.
- [4] M. Heydt, A. Rosenhahn, M. Grunze, M. Pettitt, M.E. Callow, and J.A. Callow, "Digital in-line holography as a three-dimensional tool to study motile marine organisms during their exploration of surfaces," *Journal of Adhesion*, vol. 83(5), pp. 417–430, 2007.
- [5] M. Heydt, P. Divos, M. Grunze, and A. Rosenhahn, "Analysis of holographic microscopy data to quantitatively investigate three-dimensional settlement dynamics of algal zoospores in the vicinity of surfaces," *European Physical Journal E*, vol. 30(2), pp. 141–148, 2009.
- [6] J. Sheng and et al., "Digital holographic microscopy reveals prey-induced changes in swimming behavior of predatory dinoflagellates," *Proceedings of the National Academy of Sciences of the United States of America*, vol. 104(44), pp. 17512–17517, 2007.
- [7] J. Sheng, E. Malkiel, J. Katz, J.E. Adolf, and A.R. Place, "A dinoflagellate exploits toxins to immobilize prey prior to ingestion," *Proceedings of the National Academy of Sciences of the United States of America*, vol. 107(5), pp. 2082–2087, 2010.
- [8] W. Xu, M.H. Jericho, H.J. Kreuzer, and I.A. Meinertzhagen, "Tracking particles in four dimensions with in-line holographic microscopy," *Optics Letters*, vol. 28(3), pp. 164–166, 2003.

- [9] N.I. Lewis and et al., "Swimming speed of three species of *Alexandrium* (*Dinophyceae*) as determined by digital in-line holography," *Phycologia*, vol. 45(1), pp. 61–70, 2006.
- [10] L. Leal-Taixé, M. Heydt, A. Rosenhahn, and B. Rosenhahn, "Automatic tracking of swimming microorganisms in 4D digital in-line holography data," *Workshop on Motion and Video Computing*, vol. WMVC'09 (IEEE), pp. 1–8, 2009.
- [11] L. Leal-Taixé, M. Heydt, S. Weisse, A. Rosenhahn, and B. Rosenhahn, "Classification of swimming microorganisms motion patterns in 4D digital in-line holography data," *32nd Annual Symposium of the German Association for Pattern Recognition (DAGM)*, vol. 6376, pp. 283–292, 2010.
- [12] N. Hasler, B. Rosenhahn, T. Thormaehlen, M. Wand, J. Gall, and H.-P. Seidel, "Markerless motion capture with unsynchronized moving cameras," *CVPR*, 2009.
- [13] R. I. Hartley and A. Zisserman, *Multiple View Geometry in Computer Vision*, Cambridge University Press, ISBN: 0521540518, second edition, 2004.
- [14] W. Blaschke, *Kinematik und Quaternionen, Mathematische Monographien*, 4. Deutscher Verlag der Wissenschaften, 1960.
- [15] HW. Kuhn, "The hungarian method for the assignment problem," *Nav. Res. Logist.*, vol. 2, pp. 83–87, 1955.
- [16] J. Pineda, D. Riebensahm, and D. Medeiros-Bergen, "Semibalanus balanoides in winter and spring: larval concentration, settlement, and substrate occupancy," *Marine Biology*, vol. 140, pp. 789–800, 2002.
- [17] J. O. Bjørndal, "Marine aquarium blog," <http://www.jonolavsakvarium.com/blog/200805/barnacle01.jpg>, [22.06.2011].